THE JOURNAL OF PHYSICAL CHEMISTRY B

ARTICLE

pubs.acs.org/JPCB

Convective Mixing Induced by Acid−Base Reactions

C. Almarcha,[*,†,‡] Y. R'Honi,[‡] Y. De Decker,[‡] P. M. J. Trevelyan,[‡,§] K. Eckert,[⊥] and A. De Wit[‡]

[†]IRPHE, UMR 6594, CNRS, Université d'Aix-Marseille 1, 49, rue F. Joliot Curie, 13384 Marseille, France

[‡]Nonlinear Physical Chemistry Unit, CP 231, Faculté des Sciences, Université Libre de Bruxelles (ULB), Campus Plaine, 1050 Brussels, Belgium

[§]Division of Mathematics and Statistics, Faculty of Advanced Technology, University of Glamorgan, Pontypridd, CF37 1DL, United Kingdom

[⊥]Technische Universität Dresden, Institute for Fluid Mechanics, D-01062 Dresden, Germany

ABSTRACT: When two miscible solutions, each containing a reactive species, are put in contact in the gravity field, local variations in the density due to the reaction can induce convective motion and mixing. We characterize here both experimentally and theoretically such buoyancy-driven instabilities induced by the neutralization of a strong acid by a strong base in aqueous solutions. The diverse patterns obtained are shown to depend on the type of reactants used and on their relative concentrations. They have their origin in a combination of classical hydrodynamic instabilities including differential diffusion of the solutes involved while temperature effects only play a marginal role.

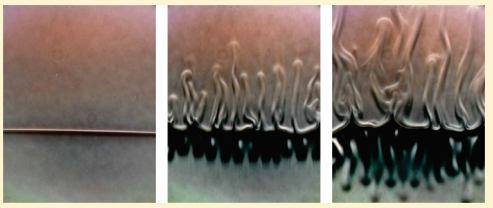

INTRODUCTION

In reactive systems, forced convection is an efficient way to mix reactants and hence increase the reaction rate. This is of particular importance in chemical engineering processes. Conversely, one can address the question: how can chemical reactions influence natural convection or even be at the very source of hydrodynamic motion? These issues are at the heart of numerous applications in combustion,[1,2] polymer processing,[3,4] extraction techniques,[5,6] microfluidic devices,[7−9] bioconvection,[10] traveling fronts,[11−13] and CO_2 sequestration,[14,15] to name a few.

To answer such questions, experimental studies have for instance investigated chemically driven convective mixing and enhanced extraction from one phase to another, induced by reactions between reactants initially contained separately in immiscible solvents.[5,16−18] In that case, it has been shown that the flow around the interface and within the bulk solutions result from (i) the coupling between transfer of chemical species at the interface, (ii) changes by the reaction of the density of the solutions which can trigger buoyancy-driven convective motions, and (iii) reaction-induced Marangoni effects, that is, fluid motion generated by surface tension changes at the immiscible interface. The situation is therefore quite complex, and even if theoretical studies[19−21] provide some help in understanding the influence of the various parameters, there is a need to gain insight also into simpler situations where some of the various effects are isolated. In this regard, the use of miscible solvents removes the influence of both transfer rate and Marangoni effects and allows one to separately analyze the influence of purely buoyancy-driven convection.

For such miscible solvents, it has been shown experimentally that putting in contact aqueous solutions of an acid and of a base in the gravity field allows one to observe a wealth of beautiful convective patterns and instabilities.[22−25] More specifically, ascending plumes can develop above the reaction front when a solution of hydrochloric acid is put on top of a denser miscible equimolar aqueous solution of sodium hydroxide.[23] The patterns are different in presence of a color indicator,[22] indicating that this species is not neutral to the convective dynamics.[24]

In this context, it is of interest to analyze such miscible systems in which a simple acid−base reaction takes place to understand the various possible buoyancy-driven instabilities induced by the presence, in aqueous solutions, of the neutralization reaction $H^+ + OH^- \rightarrow H_2O$. To do so, we study experimentally chemically driven convective motions arising when putting in contact an aqueous solution of a strong acid on top of a denser aqueous solution of a strong base in the gravity field. We explain the influence on the dynamics of changing the type of reactants used and their concentrations. In a first part, we vary the type of counterion in the basic solution at fixed concentrations. We next vary the ratio in concentrations between the acid and the base solutions for a specific acid−base couple. Finally, we show how one can rationalize all of the complex behaviors observed simply in terms of the concentrations $[i]$ of species I, their diffusion coefficients D_i, and their solutal expansion coefficients α_i.

EXPERIMENTAL SETUP

The experimental setup[26] consists in a vertically oriented Hele-Shaw cell, that is, two glass plates 3.6 cm wide, 6.2 cm tall, and 10 mm thick separated by a thin gap width $h = 0.57$ mm, filled with the reactants. The cell has two injection holes, respectively on top and bottom, which are connected to syringes by 1 mm diameter tubes. An exhaust hole is located on each lateral side. The flat horizontal initial contact line between the two miscible reactant solutions is obtained by the following procedure: the cell

Received: March 8, 2011
Revised: July 7, 2011
Published: July 11, 2011

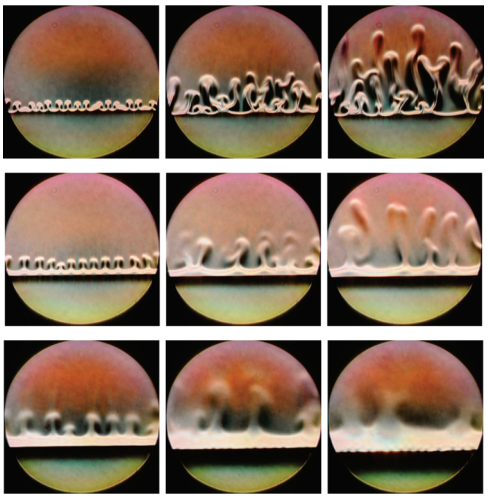

Figure 1. Buoyancy-driven instabilities of the miscible interface between a solution of HCl 1 mol/L (±0.2%) on top of a solution of MeOH with same concentration. Me stands for Li, Na, and K. The field of view is 3 cm. (top) LiOH shown at t = 20 s, 1 min, and 2 min from left to right; (middle) NaOH at t = 80, 200, and 300 s; (bottom) KOH at t = 4, 10, and 20 min.

is first totally filled up in the vertical position with the lower reactant, injected through the bottom hole. When all of the air is evacuated from the cell and the tubes, the upper reactant solution is injected from the upper hole to fill the upper half of the cell. The excess of liquid is evacuated by the exhaust side holes. The upper and lower reactants are then continuously injected from the top and bottom so that a thin horizontal boundary line connecting the two exhaust sites appears. The thickness of this horizontal layer decreases when the speed around the stagnation point in the middle of the cell increases. This thickness is indeed given by the points at which the diffusive flux of the species is balanced by their convective flux due to injection. No instability develops yet as the injection velocities are typically 2 orders of magnitude larger than the velocities induced by destabilization. The injection is then stopped, and the dynamics is allowed to evolve from this initial condition. Visualizations are performed by the Schlieren technique. For the specific HCl/NaOH acid base pair, it has been shown theoretically that the characteristic wavelength of the convective pattern and its onset time both scale with the concentration, while the nature of the instability only depends on the concentration ratio $r = [b]_0/[a]_0$ between the acid and the base initial concentrations.[23] All experiments presented in the following will therefore fix the concentration $[a]_0$ of the HCl solution on top to 1 mol/L.

EXPERIMENTAL RESULTS

Phenomenology of the Dynamics in HCl/MeOH Systems. Figure 1 (middle) shows the typical dynamics observed when putting a solution of HCl on top of an equimolar denser NaOH one in the absence of any color indicator and using water as the solvent: quite rapidly, buoyant plumes start rising above the initial contact line, as detailed in previous studies.[23] Some of the fingers merge, and a general coarsening toward larger fingers is observed. In some cases, a finger can also split into two. Below the initial contact line, no convective motions are observed. The reaction front, defined as the location where a maximum of product is generated, can be seen as a sharp contrast between the black and the white zones moving slowly as an unperturbed planar line in the lower alkaline zone.

Table 1. Summary of the Possible Buoyancy-Driven Instabilities When, in the Gravity Field, an Upper Solution of Density ρ_u Containing a Solute with Diffusion Coefficient D_u Overlies a Lower Solution of Density ρ_l Where the Solute Has a Diffusion Coefficient D_l

instability	condition
RT	$\rho_u > \rho_l$
DLC	$D_u > D_l$
DD	$D_u < D_l$

To understand the origin of the fingers observed, it is useful to recall that previous results[23] suggest that buoyancy instabilities in reactive solutions can be understood in terms of the following instabilities found in the nonreactive case:[27,28] when a denser solution lies on top of a less dense one in the gravity field, a Rayleigh−Taylor (RT) instability can develop and deform the miscible interface into interpenetrating "fingers". A double diffusive (DD) fingering can also appear if the solute in the lower denser solution diffuses faster than the solute in the upper solution. On the contrary, if the solute in the upper less dense solution diffuses faster than the solute in the denser lower solution, a diffusive layer convection (DLC) may be observed. Convection results in that case from the build-up in time because of differential diffusion effects of nonmonotonic density profiles[29,30] where locally adverse gradients (dense over less dense) trigger convective motions. Table 1 summarizes these various possibilities. These three types of hydrodynamic instabilities can be locally recovered in the reactive case as sources of convection around the reaction front, depending on the physical properties of the species as shown in the following.

In the case of HCl/NaOH, it has been shown theoretically[23] that the rising plumes are due to a DLC mechanism because we initially have a stratification of an upper less dense solution of fast diffusing acid on top of a lower denser solution of base[23] (case $D_u > D_l$ of Table 1). While such a DLC mechanism is known to produce convection at symmetric distances above and below the contact line in nonreactive systems,[27] it is important to note that the chemical reaction breaks the symmetry of the pattern: DLC convection is observed in this reactive system only ABOVE the initial contact line, while the acid diffusing downward (the accumulation of which would be responsible for convection in the lower layer in nonreactive systems) is here replaced by the salt. Let us now analyze how these known results are affected by changes in the nature of the base and in the relative concentration of the acid and of the base.

Effect of the Counterion. We first investigate experimentally the effect of changing the counterion of the hydroxide in the lower basic solution keeping the concentration ratio r fixed to one (stoichiometric configuration). Table 2 summarizes the physical properties of HCl, of the bases used and of the related salts produced by giving the solutal expansion coefficients defined as $\alpha_i = (1/\rho_o)(\partial\rho_d/\partial[i])$, and the ratios of diffusion coefficients $\delta_B = D_B/D_A$ and $\delta_C = D_C/D_A$ at a reference temperature of T_0 = 293 K. Here ρ_d and ρ_o are the dimensional density of the solution and of the pure solvent (water here), respectively. It is seen that, going down the alkaline column, we have

$$\alpha_{LiOH} < \alpha_{NaOH} < \alpha_{KOH} < \alpha_{CsOH} \quad (1)$$

Table 2. Expansion Coefficients α_i, Diffusion Coefficients D_i, Expansion Coefficient Ratio $R_i = \alpha_i/\alpha_A$, and Ratio of Diffusion Coefficients $\delta_i = D_i/D_A$ of the Involved Chemical Species (From Reference 35)

species i	α_i [10^{-2} L/mol]	D_i [10^{-9}m^2/s]	R_i	δ_i
HCl (A)	1.8	3.336	1.0	1.0
LiCl (C_1)	2.4	1.366	1.4	0.41
LiOH (B_1)	2.7	1.722	1.5	0.52
NaCl (C_2)	4.1	1.611	2.3	0.48
NaOH (B_2)	4.4	2.129	2.5	0.64
KCl (C_3)	4.7	1.994	2.7	0.60
KOH (B_3)	4.9	2.855	2.8	0.86
CsCl (C_4)	12.8	2.044	7.2	0.62
CsOH (B_4)	13.0	2.958	7.3	0.89

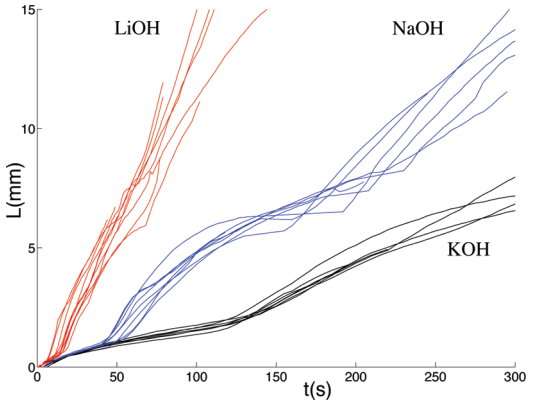

Figure 2. Temporal evolution of the highest plume position L for 1 mol/L HCl on top of 1 mol/L MeOH.

This can be related to the increasing weight of the alkaline counterion. In parallel, we also have

$$D_{LiOH} < D_{NaOH} < D_{KOH} < D_{CsOH} \quad (2)$$

The LiOH ion pair diffuses the slowest because the positive charge of the alkaline cation is acting on the smallest ion radius and creates therefore the largest solvation shell. In effect the solvated ion pair is of decreasing radius along the alkaline column which explains the increasing effective diffusion coefficient.

To compare the influence of a change in the nature of the base, we have first compared dynamics using a fixed 1 mol/L solution of HCl on top of denser 1 mol/L solutions of lithium, sodium, potassium, or cesium hydroxide, respectively. While no convection is observed with the CsOH solution, convective patterns quickly appear when LiOH, NaOH, and KOH are put in contact below the equimolar HCl solution, as shown in Figure 1. In these three cases, plumes grow upward in the upper solution, on top of the reaction front traveling in the lower layer. The reaction front remains flat with NaOH and KOH solutions, but it is perturbed with LiOH because of the intense convection in the upper layer. As a consequence, the reaction front moves faster downward for LiOH. We note that convection is less and less efficient and appears later when increasing the atomic weight of the hydroxide counterion. Figure 2 shows the temporal evolution of the position L of the upper perturbation in the refraction index of the solution with regard to the initial contact line position.

Figure 3. Dynamics of the interface between a solution of 1 mol/L HCl on top of a solution of 0.4 mol/L NaOH with the same density. A snapshot was taken every minute. The field of view is 3 cm.

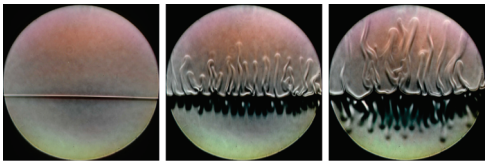

Figure 4. Dynamics of the interface between a solution of 1 mol/L HCl on top of a solution of 0.137 mol/L CsOH with the same density. A snapshot was taken every minute. The field of view is 3 cm.

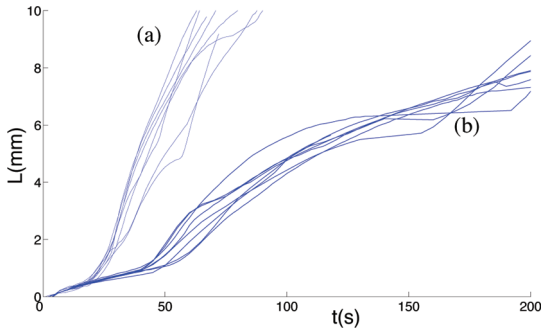

Figure 5. Temporal evolution of the highest plume position L for 1 mol/L HCl on top of NaOH, with the same density (a) and with the same concentration (b).

It typically represents the location of the plume tip of the highest finger. Each curve stands for one experiment. To compare different experiments for various values of the parameters, for which the initial contact line position can hardly be controlled, the reference positions were aligned at times 3, 10, and 20 s within the diffusive regime for each series of experiment with LiOH, NaOH, and KOH, respectively. For all species, we observe first a diffusive regime in which the refraction index isocontours are flat and the distances between them grow like the square root of time. In a second regime, plumes appear and grow upward. Their velocity first quickly increases and then slows down because of transverse diffusion, before increasing again due to feeding or merging of one plume with another plume. The maximum velocity reached by the plumes decreases with the counterion weight while their time of onset increases. We can conclude that the intensity of convection decreases along the alkaline column and is less effective for bigger counterions.

Effect of Relative Acid and Base Concentrations. Keeping the concentration of HCl at 1 mol/L, we also performed experiments where the concentration of the basic solution is decreased to decrease the density of the lower solution down to that of the upper one. We observe that convection increases when decreasing the lower solution concentration as seen when comparing Figures 3 and 4 with Figure 1. The plume positions in the course of time are compared in Figure 5 for a bottom solution of 1 mol/L

NaOH or for NaOH with a density close to the upper HCl 1 mol/L solution (≈ 1.016 g cm^{-3}). There is a clear increase in the plume velocity and a decrease in the time of their appearance when decreasing the lower solution concentration.

For CsOH, decreasing the concentrations to obtain isopycnic reactant solutions allows us to observe destabilization as seen in Figure 4, while the interface was stable for equimolar solutions. Moreover, we observe that, in this case, fingers also appear in the lower layer.

All of these observations are explained in the following section.

INTERPRETATION OF EXPERIMENTAL RESULTS

As we use a strong acid and a strong base in water, all of the species, including the salt formed by the reaction, are fully dissociated in ions. In the hydroxide solution, we define Me^+ as the counterion of OH^- where $Me^+ = Li^+$, Na^+, K^+, or Cs^+. In the acidic solution, the negative counterion of H^+, which is here Cl^-, is denoted by γ^-. Due to local electroneutrality, we consider in a first approximation that each ion diffuses with a counterion, forming an ion pair $Me^+\gamma^-$.

On the basis of this assumption, we can express the density as a Taylor expansion (assuming diluted solutions) as

$$\rho_d = \rho_o[1 + \alpha_A[a] + \alpha_B[b] + \alpha_C[c] + \alpha_T(T_d - T_o)] \quad (3)$$

where $\alpha_T = (1/\rho_o)(\partial\rho_d/\partial T)$ is the thermal expansion coefficient, T_d the dimensional temperature of the solution, and T_o the reference temperature at which the values of Table 1 are given. $[a]$, $[b]$, and $[c]$ are the concentrations of the acid A, base B, and salt C which are the pairs $H^+\gamma^-$, Me^+OH^-, and $Me^+\gamma^-$, respectively. Defining dimensionless concentrations $(a, b, c) = ([a], [b], [c])/[a]_0$ and temperature $T = (T_d - T_0)/(|\Delta H|[a_0]/\rho_0 C_p)$, we next construct the dimensionless density profile $\rho(x) = (\rho_d - \rho_0)/\rho_0\alpha_A[a]_0$ along the vertical coordinate to gain insight into possible causes of convection. Explicitly, we obtain:

$$\rho = a + R_B b + R_C c + R_T T \quad (4)$$

where $R_B = \alpha_B/\alpha_A$ and $R_C = \alpha_C/\alpha_A$ are the ratios of solutal expansion coefficients α_i given in Table 2 while the thermal expansion ratio $R_T = \alpha_T|\Delta H|/\alpha_A\rho_0 C_p$. For pure water, the specific heat $C_p \approx 4.18$ kJ/(kg K), $\rho_0 \approx 0.998$ kg/L, the thermal expansion coefficient $\alpha_T = -2.1 \times 10^{-4}$ K^{-1} while the enthalpy of the neutralization reaction is $\Delta H \approx -57$ kJ/mol. We get $R_T = -0.16$, that is, the influence of exothermicity on expansion is an order of magnitude smaller than solutal effects. Heat also diffuses faster than mass, giving a Lewis number $Le = D_T/D_A = 40$ with $D_T = 1.35 \times 10^{-7}$ m^2/s.

On the basis of the above numbers, we can understand the relative importance of density- and diffusion-related effects in the dynamics. Let us review them consequently.

Solutal Density Effects. To avoid a straightforward RT instability of the initial stratification of the reactants, we chose here to always start with a lower reactant solution denser than the upper reactant solution. The species diffusing up from the lower solution (OH^- and Me^+ in the present study) have therefore a stabilizing contribution to density. This first stabilizing contribution can however be counterbalanced by the destabilizing effect of the reaction on density. Indeed, as the volume occupied by the H_2O molecule is larger than the sum of the volume of both H^+ and OH^-, which can be checked by verifying that $R_C < R_A + R_B$ in Table 2, the reaction $H^+ + OH^- \rightarrow H_2O$ induces a local decrease of the solution density.[31] If this second effect is more important than the first one, the reaction zone becomes less dense than its surroundings which can induce locally RT buoyant plumes rising upward in the upper solution where the denser reactant acid solution overlies the less dense reaction zone, as illustrated in Figure 1 (top). The criterion for onset of this solutal instability depends therefore on the relative density of the acid solution versus that of the product one. In the very specific case $\delta_B = \delta_C = 1$ of contact between reactants with equal initial concentration $[a]_o = [b]_o$, the concentration of the product in the reaction zone is half of it,[31] that is, $[c] = [a]_o/2$. As a consequence, eq 4 shows that, if the pure acid solution has a dimensionless density $\rho = 1$, the pure base has a density $\rho = R_B$, while the density at the contact point is equal to $R_C/2$. Hence, in this specific case, the stratification of the acid over the salt produced in the reaction zone is RT unstable as soon as $R_C < 2$. An inspection of Table 2 shows that this is the case for LiCl only suggesting that, if all of the diffusion coefficients were equal, the RT instability would be responsible for the upward moving fingers in the dynamics of HCl put on top of LiOH. For all other alkalines, $1 < R_C/2$ here, and a RT mechanism is excluded in the upper zone when $\delta_i = 1$. Below the reaction zone, a RT instability is not possible where the product overlies the base because we can never have $R_C/2 > R_B$, as $R_C < R_A + R_B$ (expansion of the solution due to reaction) and $R_A < R_B$ (acid solution initially less dense than basic solution). In the more general case of unequal diffusion coefficients,[32] it is known[33] that the concentration at the stationary reaction front is $c = [a]_o/(4\delta_c)^{1/2}$ so that the dimensionless density at the reaction front is equal to $R_C/(4\delta_c)^{1/2}$. The reaction zone is therefore less dense than the upper solution provided that $R_C < (4\delta_c)^{1/2}$, which is a sufficient criterion for RT instability in the upper layer. In this expression, we clearly see that the diffusion coefficients can also play a role, which is explained in the following paragraph.

Differential Diffusion Effects. From the perspective of diffusive effects, as H^+ is the fastest diffusing cation and OH^- the fastest diffusing anion, the product of the reaction always diffuses slower than both of these reactants (the diffusion coefficient of the electrolyte is computed as the harmonic mean of mobilities). As a consequence, the reaction zone provides a slow diffusing product sandwiched between the acid and the basic regions containing faster diffusing species.[32] A DLC mechanism[27] can hence take place between the faster diffusing acid overlying the slower diffusing product (see Table 1), creating plumes that rise up in the upper solution. A DD instability can appear in the density stable lower part because the slower diffusing product overlies the faster diffusing base, creating falling fingers in the lower solution. An illustration of both such differential diffusion effects is given in Figure 4 for CsOH. The DLC instability acts above the reaction front and the DD instability effect below it. DLC is induced by the fast diffusion of the acid downward that gives a depletion zone. However, DD fingers are obtained in the lower part only if the difference in diffusion coefficient between the involved species is large enough (like for CsOH, Figure 4) and the height of the stable barrier below the reaction zone is not too large.

DENSITY PROFILES

To better understand the relative role of density and diffusive effects observed when varying the nature of the species used and their concentration, we compute one-dimensional (1D)

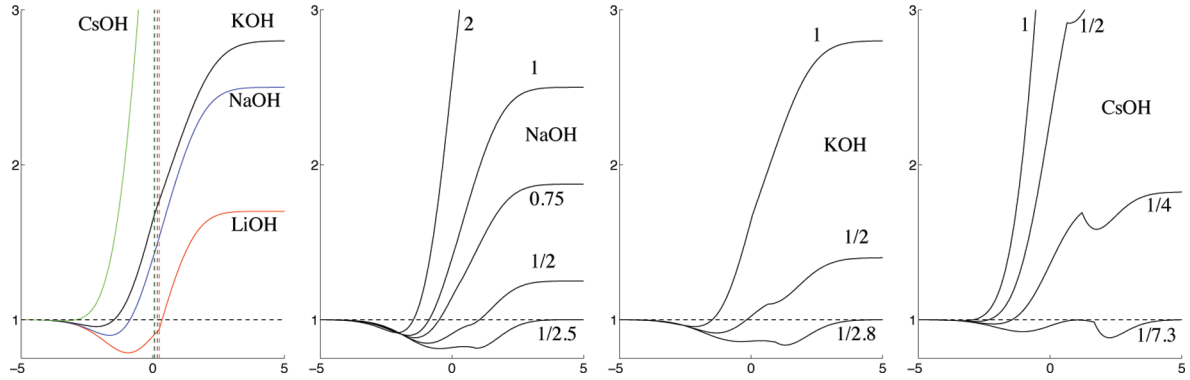

Figure 6. Dimensionless density profiles $\rho(\xi)$ for 1 mol/L HCl on top of (a) 1 mol/L MeOH; (b–d) variable concentration ratios r.

reaction-diffusion density profiles $\rho(\xi)$ along the nondimensional vertical coordinate $\xi = x/(D_A t)^{1/2}$. To do so, we insert large time asymptotic reaction-diffusion concentration profiles of an A + B → C reaction front[33,34] inside $\rho(\xi)$ using eq 4. It is justified to use such long time asymptotic profiles here as we deal with quasi-instantaneous acid–base reactions. The initial contact zone of the solution is at $\xi = 0$.

Equimolar Solutions. The density profiles are shown in Figure 6a for the four different hydroxide solutions and equimolar initial concentrations of acid and base ($r = 1$). For each case, the density ranges from 1 in the pure acid part to R_B in the pure basic zone. The reaction front position is represented by a vertical dotted line with same color. We see that changing the hydroxide counterion going down the alkaline column in the periodic table of elements (from Li^+ to Cs^+) has two consequences. First, as the related solutal expansion coefficient increases, the density of the equimolar lower basic solution also increases (in the $\xi > 0$ zone) leading to an increasingly larger stabilizing density barrier below the reaction zone. In parallel, going from Li^+ to Cs^+, the corresponding hydroxide diffuses faster toward the upper region leading to a less pronounced local minimum in the density above the reaction zone and therefore to less intense convection. These two effects are both responsible for a decrease of the convection when going down the alkaline column as seen in Figure 2. For CsOH, the diffusion of this base and its density at 1 mol/L are both large enough to compensate for the diffusion of the acid downward so that the minimum in density is tiny, which explains why no convection is observed for a stratification of HCl above an equimolar CsOH solution.

Isopycnic Solutions. At the same concentration, the HCl solution is less dense than the alkaline one. To decrease the stabilizing influence of the denser barrier below the reaction zone, we have progressively diluted the lower alkaline solution. The effect of this dilution is reported for NaOH, KOH, and CsOH in Figure 6b, c, and d, respectively. On Figure 6b, we see that decreasing the concentration of NaOH from 2 mol/L to $(1/R_B)$ mol/L (for which we get the isopycnic case where both solutions have the same density) decreases the height of the stabilizing density barrier in the lower layer and enhances the intensity of the local minimum in the density profile. This induces more intense convection appearing faster as can be appreciated when comparing Figure 1 (middle) for 1 mol/L NaOH with Figure 3 for 0.4 mol/L NaOH (i.e., for $r = 1/R_B$). In the lower solution, a flat reaction front is observed as long as it propagates in the stable density stratification like in Figure 1, while this reaction front is strongly deformed by convection if this stable barrier does not exist any longer like in Figure 3.

It has to be noted that two local minima are always present in $\rho(\xi)$ for solutions close to isodensity. They both come from the fact that the product, with the maximum concentration at the reaction front, diffuses less than the upper and lower reactants. When reactants do not have the same density, the lower minimum may be masked by the lower density gradient. Anyway, as one can see in Figure 6d for HCl on top of CsOH with the same density, two very distinct local minima appear in the isopycnic case, which explains the appearance of DD fingering in the lower layer, in addition to diffusive layer convection in the upper layer, as reported in Figure 4.

Thermal Effects. The above discussion does not take thermal effects due to the exothermicity of the neutralization reaction into account. Let us show that such effects are of small amplitude and do not change the conclusions anyway. Indeed, as the density of water decreases with temperature (at least above 4 °C where experiments are performed at 20 °C), the volume of the hotter reaction zone expands as far as the thermal contribution to density concerns, allowing thermal plumes due to a Rayleigh–Bénard mechanism (heating from below) to appear. Such a temperature effect is therefore reinforcing the RT or DLC mechanism acting in the upper layer leading to rising fingers.

In the lower layer, the temperature stratification is stable as we have a hot reaction zone on top of a colder alkaline region. Instability involving heat could thus only come from potential differential diffusion effects of heat versus mass. Such effects are typically observed when a hot and solute-heavy solution overlies a colder solute-poor zone, the total density profile being stable.[28] This effect is here more tricky as, in addition to heat, two couples of solutes are present on each side of the reaction front. Heat cannot have a differential diffusion interaction with the reactants A and B, as their contribution all implies a decrease in the density when approaching the reaction front. The only effect can therefore appear between competitive contribution to the density of the product and of the temperature. As heat diffuses faster than the product, a DD-like instability can appear under the reaction front where the hot product-rich zone overlies the colder product-poor lower part, and a DLC-like instability can appear on top of the reaction zone. Hence, the differential diffusion thermal effects are similar and superimposed to the solutal differential diffusion effects. In conclusion, the thermal effect will affect the flow in the same way as the solutes. It cannot add another scenario of destabilization. It can just increase the strength of the appearing instabilities.

To measure the relative magnitude of temperature and solutal effects in the strength of the convection, we measured the

temperature contribution to the variation of ρ and found it was negligible. Exothermicity indeed has a weak influence on destabilization as can be understood when comparing the strength of solutal versus thermal convective forces quantified for porous media or thin[36] Hele−Shaw cells by Rayleigh−Darcy numbers $R_a = \alpha_A a_0 g l_a h^2/(12\nu D_A)$ for species A and $R_T = \alpha_T \Delta T g l_T h^2/(12\nu D_T)$ for temperature, where the characteristic lengths l_a and l_T for acid and temperature profiles, respectively, increase in time like $(D_A t)^{1/2}$ and $(D_T t)^{1/2}$. In the case of 1 mol/L solution of HCl on top of an equimolar solution of NaOH, the maximum value of the increase in temperature in the nonconvective regime is found to be $\Delta T \approx 0.96$ K, imposing a maximum decrease in the density $\Delta\rho/\rho \approx 2 \times 10^{-4}$. The ratio R_T/R_a is estimated to be $\alpha_T \Delta T/\alpha_A a_0 (\mathrm{Le})^{1/2} \approx 1.8 \times 10^{-3}$. Thus thermal effects can safely be neglected in the destabilization, and this conclusion is all the more true in thin Hele−Shaw cells if heat losses are observed through the glass plates.

In thicker cells or three-dimensional (3D) tanks, a similar analysis can be conducted using Rayleigh numbers $R_a' = \alpha_A a_0 g l_a^3/(\nu D_A)$ and $R_T = \alpha_T \Delta T g l_T^3/(\nu D_T)$ which shows that $R_T/R_3' = R_T/(R_a \mathrm{Le}) \approx 7 \times 10^{-2}$. Thermal effects remain thus at least an order of magnitude smaller than the solutal effects. This is an interesting quantitative conclusion[23] as the exothermic character of the acid−base system could have been thought a priori to play a key role.

CONCLUSIONS

In conclusion, we have experimentally shown and theoretically discussed the various possible convective regimes that can be triggered by acid−base reactions when a less dense acid solution lies on top of a denser alkaline one in the gravity field. We showed that, in the case of strong acids and bases, the possible dynamics are a composition of only two asymptotic cases. The first one is a local RT instability above the reaction zone induced by products less dense than the upper acid solution. Plumes are then observed in the upper zone. The other possible instability mechanism results from a composition of differential diffusion instabilities, DLC above the reaction front and DD under the reaction front, induced by the fact that the product diffuses slower than the reactants. It has to be noted that interchanging the acid and the base (denser acid under lighter base) would lead to analogous results. We also explained that thermal effects are a second-order correction acting the same way as solutal effects. Hence, convection can result either from density effects leading to plumes in the upper solution only, or from differential diffusive effects, leading to fingers in the lower solution and plumes on top. As the characterization of the possible instability scenarios made here rely only on the computation of 1D density profiles and consideration on differences of diffusion coefficients, our results apply to both porous or nonporous media in both 2D and 3D geometries.

AUTHOR INFORMATION

Corresponding Author

*E-mail: almarcha@irphe.univ-mrs.fr.

ACKNOWLEDGMENT

We thank Prodex, FNRS, ARC-Archimedes, and DLR (50WM0638) for financial support.

REFERENCES

(1) Clanet, C.; Searby, G. *Phys. Rev. Lett.* **1998**, *80*, 3867–3870.
(2) Guahk, Y. T.; Lee, D. K.; Oh, K. C.; Shin, H. D. *Energy Fuels* **2009**, *23*, 3875–3884.
(3) Pojman, J. A.; Craven, R.; Khan, A.; West, W. *J. Phys. Chem.* **1992**, *96*, 7466–7472.
(4) Belk, M.; Kostarev, K. G.; Volpert., V.; Yudina, T. M. *J. Phys. Chem. B* **2003**, *107*, 10292–10298.
(5) Sherwood, T. K.; Wei, J. C. *Ind. Eng. Chem.* **1957**, *49*, 1030–1034.
(6) Avnir, D.; Kagan, M. *Nature* **1957**, *307*, 717–720.
(7) Grzybowski, B. A. *Angew. Chem., Int. Ed.* **2010**, *49*, 4170–4198.
(8) Kline, T. R.; Paxton, W. F.; Wang, Y.; Velegol, D.; Mallouk, T. E.; Sen, A. *J. Am. Chem. Soc.* **2005**, *127*, 17150–17151.
(9) Krishnan, M.; Agrawai, N.; Burns, M. A.; Ugaz, V. M. *Anal. Chem.* **2004**, *76*, 6254–6265.
(10) Pons, A. J.; Sagues, F.; Bees, M. A.; Sorensen, P. G. *J. Phys. Chem. B* **2002**, *106*, 7252–7259.
(11) Pojman, J. A.; Epstein, I. R. *J. Phys. Chem.* **1990**, *94*, 4966–4972.
(12) Pojman, J. A.; Epstein, I. R.; McManus, T. J.; Showalter, K. *J. Phys. Chem.* **1991**, *95*, 1299–1306.
(13) Zhivonitko, V. V.; Koptyug, I. V.; Sagdeev, R. Z. *J. Phys. Chem. A* **2007**, *111*, 4122–4124.
(14) Riaz, A.; Hesse, M.; Tchelepi, H. A.; Orr, F. M., Jr. *J. Fluid Mech.* **2006**, *548*, 87–111.
(15) Hassanzadeh, H.; Pooladi-Darvish, M.; Keith, D. W. *Energy Fuels* **2009**, *23*, 3328–3336.
(16) Eckert, K.; Grahn, A. *Phys. Rev. Lett.* **1999**, *82*, 4436–4439.
(17) Eckert, K.; Acker, M.; Shi, Y. *Phys. Fluids* **2004**, *16*, 385–399.
(18) Sczech, R.; Eckert, K.; Acker, M. *J. Phys. Chem. A* **2008**, *112*, 7357–7364.
(19) Citri, O.; Kagan, M. L.; Kosloff, R.; Avnir, D. *Langmuir* **1990**, *6*, 559–564.
(20) Bratsun, D. A.; De Wit, A. *Phys. Fluids* **2004**, *16*, 1082–1096.
(21) Bratsun, D. A.; Shi, Y.; Eckert, K.; De Wit, A. *Europhys. Lett.* **2005**, *69*, 746–752.
(22) Zalts, A.; El Hasi, C.; Rubio, D.; Urena, A.; D'Onofrio, A. *Phys. Rev. E* **2008**, *77*, 015304(R).
(23) Almarcha, C.; Trevelyan, P. M. J.; Grosfils, P.; De Wit, A. *Phys. Rev. Lett.* **2010**, *104*, 044501.
(24) Almarcha, C.; Trevelyan, P. M. J.; Riolfo, L. A.; Zalts, A.; El Hasi, C.; D'Onofrio, A.; De Wit, A. *J. Phys. Chem. Lett.* **2010**, *1*, 752–757.
(25) Tanoue, K.; Ikemoto, H.; Yoshitomi, M.; Nishimura, T. *Therm. Sci. Eng.* **2009**, *17*, 121–129.
(26) Shi, Y.; Eckert, K. *Chem. Eng. Sci.* **2008**, *63*, 3560–3563.
(27) Trevelyan, P. M. J.; Almarcha, C.; De Wit, A. *J. Fluid Mech.* **2011**, *670*, 38–65.
(28) Turner, J. S. *Buoyancy effects in fluids*; Cambridge University Press: New York, 1979.
(29) Yortsos, Y. C.; Hickernell, F. J. *SIAM J. Appl. Math.* **1989**, *49*, 730–748.
(30) Loggia, D.; Rakotomalala, N.; Salin, D.; Yortsos, Y. C. *Europhys. Lett.* **1995**, *22*, 633.
(31) Rongy, L.; Trevelyan, P. M. J.; De Wit, A. *Phys. Rev. Lett.* **2008**, *101*, 084503.
(32) Rongy, L.; Trevelyan, P. M. J.; De Wit, A. *Chem. Eng. Sci.* **2010**, *65*, 2382–2391.
(33) Sinder, M.; Pelleg, J. *Phys. Rev. E* **2000**, *62*, 3340–3348.
(34) Galfi, L.; Racz, Z. *Phys. Rev. A* **1988**, *38*, 3151–3154.
(35) *CRC Handbook of Chemistry and Physics*, 92nd ed.; CRC Press: Boca Raton, FL, 2011.
(36) Martin, J.; Rakotomalala, N.; Salin, D. *Phys. Fluids* **2002**, *14*, 902–905.